

# Power Flow Control between the Grid and Distributed Generation for Dynamic Load Variation with VSC Converter

L.Nadam<sup>1</sup>; M.Chakravarthy<sup>2</sup>; M.Manjula<sup>3</sup>

<sup>1</sup>Research Scholar, University College of Engineering, Osmania University, Telangana, India.

<sup>2</sup>Department of Electrical Engineering, Vasavi College of Engineering, Telangana, India.

<sup>3</sup>Department of Electrical Engineering, University College of Engineering, Osmania University, Telangana, India

**Abstract:-** This paper proposes a novel control method for the flow of power between utility and micro grid by controlling real and reactive power flow through back to back converter. The proposed control strategy runs in two different cases, in case 1 - real and reactive power are shared between the load and the micro grid through back to back converter. Case 2, the required load demand by the utility is first taken until the DG reaches its maximum limit. The balanced required power to the utility is only taken by the micro grid. It is also shown that voltage or frequency fluctuation in the load side has no impact on the voltage or power fluctuation. Different load variations, i.e. under, over load as well as constant load power sharing, are presented by simulating in MATLAB.

**Keywords:** - Active Power, Reactive Power, Back-to-Back converter, Micro Grid and Utility Grid.

## I. INTRODUCTION

Over the last few decades, numerous substantial blackouts have been documented in electric power networks worldwide, leading to significant economic losses in the respective regions [1-2]. Faults in power systems have various origins, spanning from localized issues initiated by transmission line failures and technical problems at power plants to widespread faults arising from unfavourable weather conditions or natural disasters. These incidents raise significant concerns, especially as essential facilities like hospitals, airports, and continuous process industries often experience prolonged disruptions, lasting from 5 to 10 hours and sometimes even longer. Additionally, the restoration of the grid often requires a significant amount of time after extensive blackouts. In some cases, even operational transmission lines may require temporary deactivation to facilitate the restoration of the grid [3]. As a result, addressing concerns about the future of power grids worldwide becomes an urgent necessity. An example of this rearrangement is the implementation of MGs, deployed in moderately insignificant topographical areas and coupled on the distribution system. MGs may operate in both GCM and IM modes. This versatility makes them well-suited for deployment in isolated areas, such as countryside zones, efficiently excluding the requirement for costly infrastructure [4]. Additionally, MG may independently disconnect from the main grid during power failure or adjacent faults. This

enhances the reliability and resilience of local systems, especially important for sensitive consumers during environmental calamities.

However, a malfunction in any renewable source might significantly impact the entire system, particularly if Energy Storage Systems (ESS) are not well-employed. MGs require sophisticated power regulation schemes to ensure efficient working and regulation of renewable sources to reach stability and other microgrid requirements. The improvement of power regulation for MGs has garnered significant concentration in the recent years, covering a range of proposed concepts, from numerical methods to novel optimization techniques.

Furthermore, optimization techniques are widely used to optimize the dispatch of renewable sources for minimizing total running expenses. A literature survey on this reveals that quite a lot of research has been undertaken in this domain. The power regulation for MGs, particularly in buildings, focuses on handling thermal energy and power distribution. In [6] concentrated on power regulation and controlling of MGs. In [7], authors evaluated power regulation for DC Microgrids. In [8] covered a wider range of optimization methods, and Al-Ismail [9] critically analyses EMCS methods. Classification of power management systems of microgrids is discussed in [10]. In [11], authors suggest a separate control plan for batteries and supercapacitors, using a Type II controller for one and a nonlinear PI controller for the other. The goal is to keep bus voltage and power quality stable during abrupt changes in power in a low-voltage DC microgrid. In [12], they introduce a secondary voltage control system in a DC microgrid to reduce sudden voltage changes caused by decentralized local power controllers in DERs. In [13], they suggest a control system for DC microgrids, where an AC voltage signal is added to the DC voltage of the microgrid, enhancing voltage regulation.

In [14], Authors propose integrating a nonlinear adaptive controller with MPPT to control the DC bus voltage during islanded operation and grid transitions in a microgrid. The importance is on selecting MPPT control to optimize the utilization of RES. Additionally, the adaptive parameters of the droop controller are optimized using sequential quadratic programming. In [15], an FOPID controller is used to control

the DC bus voltage in a hybrid microgrid designed for remote and islanded operation. In [16], an implemented control system relies on a normalized gradient adaptive regularization factor neural filter for an AC microgrid powered by a PV-BESS. The primary objective of this control strategy is to regulate the DC link voltage of the voltage source converter, ensuring optimal power extraction from the PV source.

In [17], a voltage control system is proposed as part of the secondary control stage within a distributed multi-agent system structure. This system is designed to regulate both voltage and frequency, correcting Voltage-Frequency (V-F) deviations caused by the droop controller in the primary control stage. In [18] introduced an adaptive droop-based cooperative scheme to distribute the load among BESS installed in a PV-BESS based DC microgrid. In [19] utilized a virtual impedance-based droop control to share the load among parallel voltage source inverters without the need for communication to coordinate power sharing. In [20] presented an adaptive power-sharing approach for FC and generic ESS within DC microgrids, employing the k-sharing method known for its high stability levels and minimal disruptions at the FC terminals. In [21] introduced a fuzzy adaptive compensation control to correct disproportionate reactive power sharing caused by mismatched impedances in distributed generation. The controller achieves this by dynamically adjusting the voltage reference signal of the DERs in real-time. In [22], the study focused on superimposed frequency droop control for power sharing in DC microgrids, introducing two parameters to enhance stability and address loading issues: the adaptive voltage coupling gain and adaptive amplitude of the injected AC voltage. The control of these parameters improves system operation under changing loading conditions.

The principal goal of this paper is to develop a microgrid incorporating distributed generators using power electronics. Solar and wind generation systems serve as DGs connected to the grid through back-to-back converters, facilitating bidirectional power flow control between the utility and the microgrid. The back-to-back converters are pivotal in maintaining essential frequency and power quality isolation, thereby enhancing the overall reliability and

resilience of the microgrid. The proposed setup underscores the importance of controlled and coordinated power electronics interfacing in distributed generation systems. The objectives of the paper are outlined as follows:

Investigate the use of back to back converters for power flow regulation in grid-connected DGs, with a focus on their role in facilitating bidirectional power transfer between the MG and the grid.

Design of a dynamic control with two states for efficient sharing of active and reactive power between the grid and the MG, adapting to the power requirements of the consumers.

Investigate innovative configurations of renewable sources within the microgrid to improve load-sharing in Grid-Connected Mode (GCM) and Islanded Mode (ISM), fostering resilience and optimizing resource utilization.

Evaluate the complete frequency isolation achieved by the back-to-back converters, ensuring that voltage or frequency variations in the utility grid do not impact the microgrid, thereby preserving stability.

Validate the proposed control strategy through comprehensive simulation studies using the MATLAB/SIMULINK tool, considering diverse load types, fault scenarios, and unexpected events such as fluctuations in DC side voltage and DG tripping.

## II. STRUCTURE OF THE SYSTEM

A single line diagram of the adopted system with grid, PV and wind generation systems and interconnected back to back converters are shown in Figure 1. VSC-1 and VSC-2 are two voltage source converters connected in back to back configuration for power exchange between PVGS, WGS and grid. Both these converters draw power from a DC link capacitor with a voltage denoted as  $V_c$ . Both the PVGS and WGS are linked to the microgrid using another two voltage source converters VSC-3 and VSC-4.

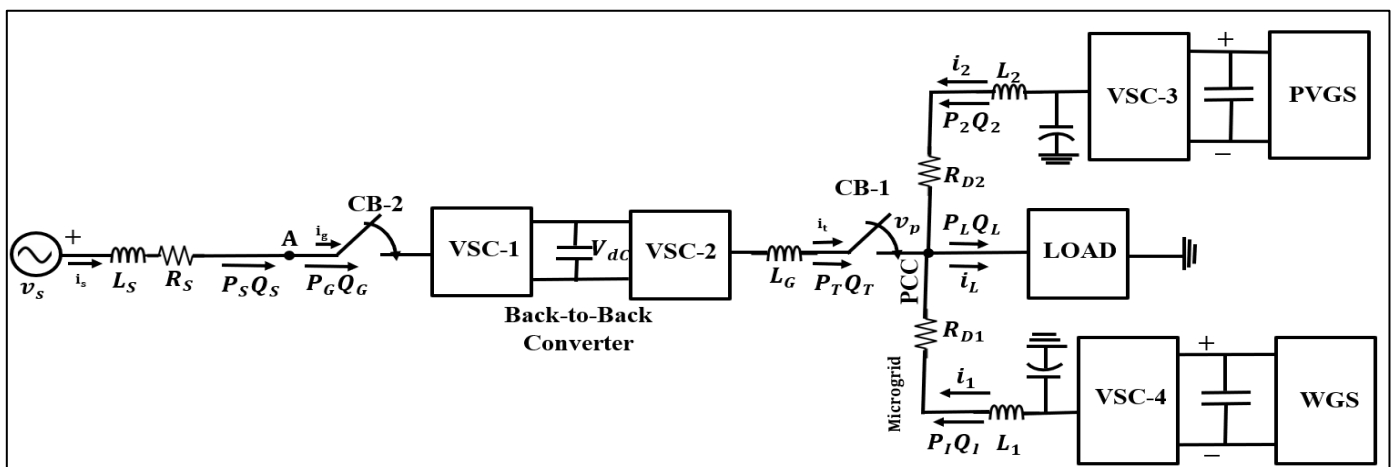


Fig 1 System Structure

The DGs' output inductances are termed as  $L_1$  and  $L_2$ .  $P_1 Q_1, P_2 Q_2$  and  $P_L Q_L$  are the real and imaginary powers at the terminals of WGS, PVGS and load respectively. Grid voltage is termed  $V_S$ .  $R_S$  and  $L_S$  are grid resistance and inductance respectively.  $R_{D1}, L_1$  and  $R_{D2}, L_2$  are the line resistance and inductances of WGS and PVGS respectively. CB1 and CB2 are the circuit breakers which connects or disconnects grid to the renewable sources.  $P_T, Q_T$  are the active and reactive power supplied from grid to the microgrid. The system can operate in two states based on the microgrid's power requirements. In State 1, a reference amount of real and reactive power which are given to control system of the back to back converter are provided by the grid to the load. Remaining power required by the load can be provided by the PVGS and WGS in proportional to their ratings. If the power demand in the microgrid exceeds the total generation capacity of both PVGS and WGS due to atmospheric disturbances state 1 is not feasible. Hence in those conditions, using State-2 control, the grid will provide the additional power required, while the DGs operate at their peak capacity.

When both DGs generate respective peak power, the MG shifts from State-1 to State-2. Though State-1 ensures a predefined power flow from the grid, State-2 offers a more consistent regulation of the back to back converter and can control significant uncertainties in both consumer side and generation side. The maximum capacity of the back to back converters depends on the peak value of the power that should be transferred through it. The peak power flow takes place when the MG experiences its highest load demand, and the DGs generate the minimum power. As a result, power flows from the grid to the microgrid. Moreover, when the DGs produce maximum power while the load demand in the

microgrid is at its minimum, it results in power flowing from the MG to the grid. The rating concern needs to be predetermined, ensuring that the MG cannot provide or allow further power than the required limit.

### III. CONVERTERS CONTROL STRATEGY

VSC-3 converter is comprising of 3 H-bridges and three Y connected 1- $\phi$  transformers and DC side is connected to the PVGS as presented in figure 2. The resistance  $R_f$  is included to consider switching and transformer losses. To mitigate switching harmonics, an LCL filter is selected. VSC-4 for WGS adopts a 6-pulse universal bridge as a converter. The converters of the back to back configuration share the same 2 universal bridges, interconnected through a DC link capacitor with a voltage of  $V_C$  as illustrated in Figure 1.

The control strategy governs all four VSCs. Each of these controllers requires its own set of instantaneous reference voltages for generating switching pulses by SPWM.

#### ➤ Reference Signal Generation for VSC-1 :

The controller angle required by VSC-1 is produced as depicted in Figure 3. Initially, the measured capacitor voltage goes through low-pass filtering, followed by a comparison with the reference DC link voltage  $V_{dc}^{ref}$ . The resulting difference between actual and reference voltage is then processed by a PI regulator to produce the reference angle  $\delta_{ref}$ .

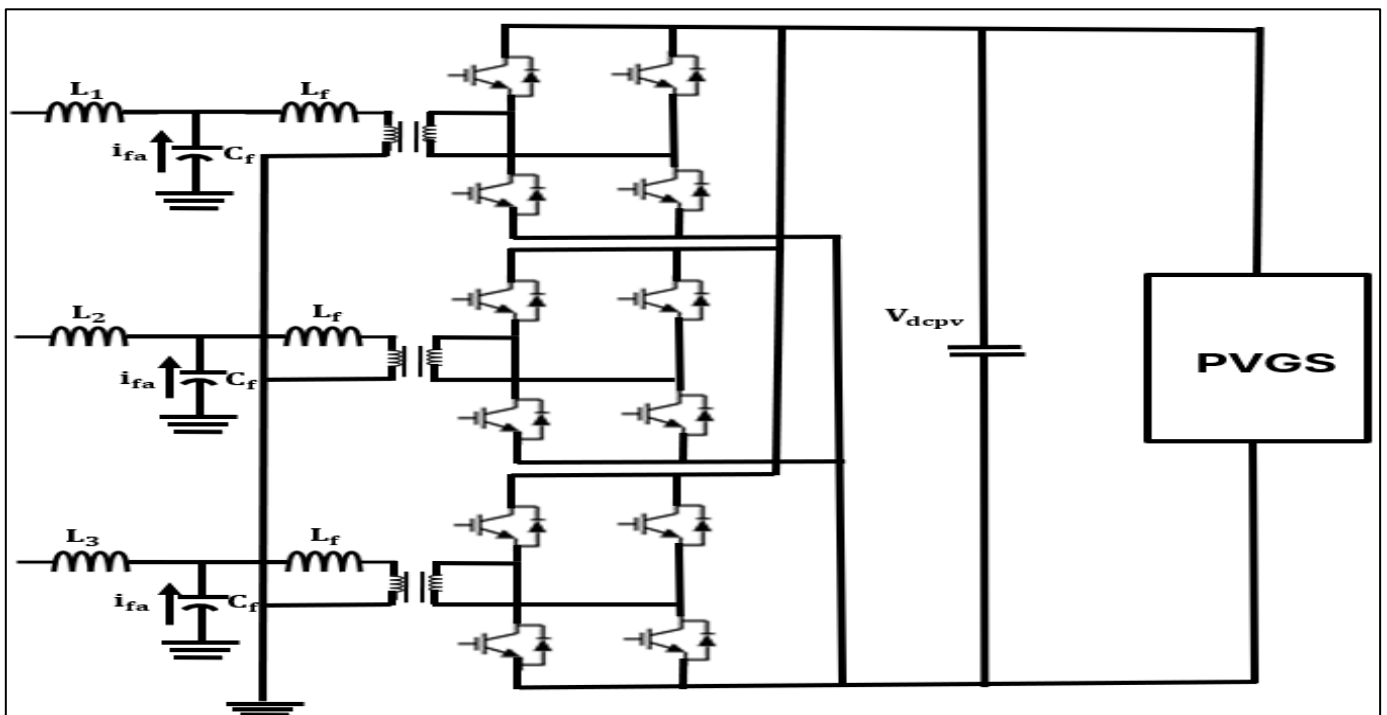


Fig 2 Converter Structure of VSC-3

Consequently, the instantaneous reference voltages of the three phases are determined using controller reference angle  $\delta_{ref}$  and voltage peak value of 1.

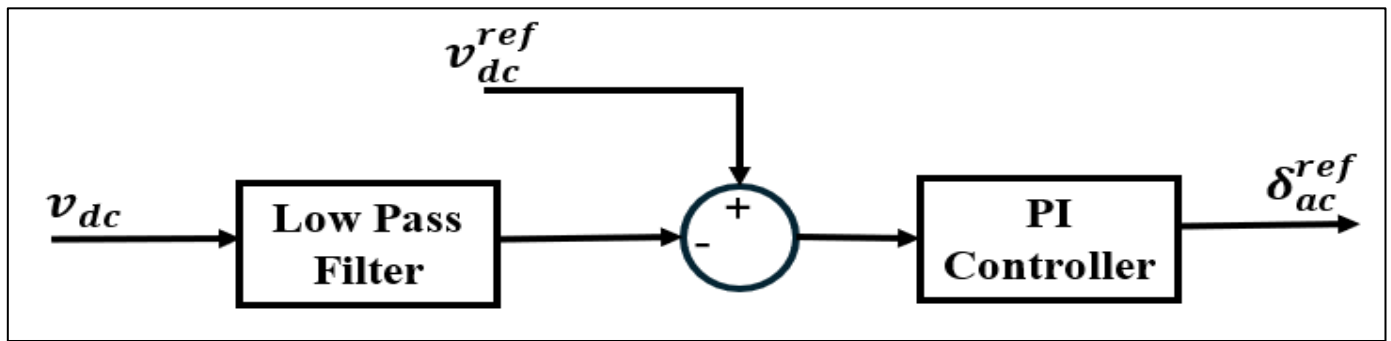


Fig 3 Reference Angle Generation for VSC-1

➤ *Reference Signal generation for VSC-2 in State-1:*

In State-1,  $P_{ref}$  and  $Q_{ref}$  are the required active and reactive powers which should be transferred between grid and MG through VSC-2. The output voltage of VSC-2 is represented by  $V_T \angle \delta_T$ , and the PCC voltage is denoted by  $V_p \angle \delta_p$ . Then the reference voltage magnitude and angle at the terminals of VSC-2 can be defined as:

$$V_T^{ref} = \frac{V_p^2 + Q_{ref} X_G}{V_p \cos(\delta_T - \delta_p)} \quad (1)$$

$$\delta_T^{ref} = \tan^{-1} \left( \frac{P_{ref} X_G}{V_p^2 + Q_{ref} X_G} \right) + \delta_p \quad (2)$$

These references are computed subject to the load demand. Reference voltage can be calculated by using  $V_T^{ref}$  and  $\delta_T^{ref}$ . And switching pulses are generated by SPWM. The sign of the reference active and reactive powers should be negative if power transfer is from MG to the grid.

➤ *Reference Signal Generation for VSC-2 in State-2:*

In State 2, if both DGs supply their maximum available power, the grid compensates for any power shortage of consumers by utilizing the back-to-back converters. Let  $P_{max}$  and  $Q_{max}$  denote the peak capacity of the back to back converters. Then reference voltage magnitude and controller angle are calculated as follows:

$$\delta_T = \delta_{max} - m_T \times (P_T - P_{max}) \quad (3)$$

$$V_T = V_{max} - n_T \times (Q_T - Q_{max}) \quad (4)$$

Here,  $V_{max}$  and  $\delta_{max}$  represent the magnitude and controller angle of the reference voltage, when supplying the maximum load.  $m_T$  and  $n_T$  are the droop coefficients and can be chosen depending on power limits of the converter.

➤ *Signal Generation for VSC-3 in State-1*

In State 1, it is considered that the grid provides a fraction of the consumers requirement, and both DGs supply and regulate the remaining requirement of the consumer. The converted voltages by VSC-3 can be controlled by considering the load proportionally of its respective DG. Controlling the real and reactive power from PVGS to the microgrid involves adjusting the magnitude and controller angle of the voltage. Injected active and reactive powers from the PVGS is given as

$$P_1 = \frac{V_1 \times V_{p1} \sin(\delta_1 - \delta_{p1})}{X_1} \quad (5)$$

$$Q_1 = \frac{V_1^2 - V_1 \times V_{p1} \cos(\delta_1 - \delta_{p1})}{X_1} \quad (6)$$

If the difference between phase angle of  $V_1$  and phase angle of  $V_{p1}$  is less than the active power provided by PVGS may be regulated by  $\delta_1$  and reactive power can be regulated by  $V_1$ . This enables the distribution of power requirements among the DGs, by adjusting the  $V_1$  and  $\delta_1$  using droop coefficients which is given as follows:

$$\delta_1 = \delta_{1rated} - m_1 \times (P_1 - P_{1rated}) \quad (7)$$

$$V_1 = V_{1rated} - n_1 \times (Q_1 - Q_{1rated}) \quad (8)$$

In this equation,  $\delta_{1rated}$  and  $V_{1rated}$  denote the rated magnitude and angle of the voltage of PVGS when it is delivering  $P_{1rated}$  and  $Q_{1rated}$  power to the load.  $m_1$  and  $n_1$  are the droop coefficients for controller angle to regulate active power and for magnitude to regulate reactive power respectively. As both DGs are converter-based, enabling instantaneous changes in the controller angle, the angle droop facilitates load sharing lacking any reduction in fundamental frequency. In a microgrid featuring frequency droop, the angular shift associated with regular load fluctuations tends to be more significant than the changes observed in the overall system fundamental frequency. If this issue is addressed with a low droop coefficient, it might result in significant frequency variations. Angle droop helps mitigate this frequency variation to some extent.

$$\delta_1 - \delta = (X_1 + X_{L1}) P_1 \quad (9)$$

$$\delta_2 - \delta = (X_2 + X_{L2}) P_2 \quad (10)$$

Where

$$X_1 = \frac{\omega L_1}{(VV_1)}, \quad X_2 = \frac{\omega L_2}{(VV_2)}, \quad X_{L1} = \frac{\omega L_{Line1}}{(VV_1)}, \quad X_{L2} = \frac{\omega L_{Line2}}{(VV_2)} \quad (11)$$

The angledroop equation of the DGs is

$$\delta_1 = \delta_{1rated} - m_1 \times (P_1 - P_{1rated}) \quad (12)$$

$$\delta_2 = \delta_{2rated} - m_2 \times (P_2 - P_{2rated}) \quad (13)$$

$$\delta_{1rated} = m_1 P_{1rated} \text{ and } \delta_{2rated} = m_2 P_{2rated}$$

Then

$$\delta_1 - \delta_2 = m_1 P_1 - m_2 P_2 \quad (14)$$

Similarly

$$\delta_1 - \delta_2 = (X_1 + X_{L1})P_1 - (X_2 + X_{L2})P_2 \quad (15)$$

Assuming a lossless system, we obtain:

$$(X_1 + X_{L1})P_1 - (X_2 + X_{L2})(P_L - P_1) = m_1 P_1 - m_2 (P_L - P_1) \quad (16)$$

$$P_1 = \frac{X_2 + X_{L2} + m_2}{X_2 + X_{L2} + m_2 + X_1 + X_{L1} + m_1} P_L \quad (17)$$

Similarly,  $P_2$  can be determined as

$$P_2 = \frac{X_1 + X_{L1} + m_1}{X_2 + X_{L2} + m_2 + X_1 + X_{L1} + m_1} P_L \quad (18)$$

The output power ratio is calculated as:

$$\frac{P_1}{P_2} = \frac{X_2 + X_{L2} + m_2}{X_1 + X_{L1} + m_1} \quad (19)$$

It is significant that the values of  $X_1$  and  $X_2$  are considerably smaller compared to the values of  $m_1$  and  $m_2$ . Moreover, considering the predominantly resistive nature of the microgrid line with minimal inductance and the significantly larger inductance

$$m_1 \gg X_1 \gg X_{L1} \text{ and } m_2 \gg X_2 \gg X_{L2} \quad (20)$$

The droop coefficients can be expressed as:

$$\frac{P_1}{P_2} \approx \frac{m_2}{m_1} = \frac{P_{1rated}}{P_{2rated}} \quad (21)$$

A high droop coefficient will consistently exert a significant impact, ensuring efficient power sharing with minimal deviation. Reactive power sharing has traditionally relied on the drop in voltage magnitude. As the converter output impedance is inductive, alterations in the controller angle have a minimal impact on sharing of imaginary power.

Therefore, PVGS can provide the required power if the terminal voltage of VSC-3 maintains the specified magnitude and angle as described in equation (5 and 6). The same approach can generate the required reference signals by VSC-4 to generate the switching pulses using SPWM

#### ➤ Signal Generation for VSC-3 in State-2

In state 2, the PV and wind systems generate their permissible peak power and remaining required power by the load can be provided by the grid. Using required active power and reactive power termed as  $P_{1avail}$  and  $Q_{1avail}$  reference voltage magnitude and controller angle can be calculated as:

$$V_1 = \frac{V_{P1}^2 + Q_{1avail} X_1}{V_{P1} \cos(\delta_{P1} - \delta_p)} \quad (22)$$

$$\delta_1 = \left( \frac{P_{1avail} X_1}{V_{P1}^2 + Q_{1avail} X_1} \right) + \delta_{P1} \quad (23)$$

### IV. SIMULATION RESULTS

Simulation studies are conducted in MATLAB/SIMULINK considering various load configurations and load-sharing scenarios. The DGs are modelled as wind and PV generation systems. Table I presents the system data. Load changes, frequency variations, and voltage disturbances at the grid side are taken into account to assess the effectiveness of the proposed strategy.

Table 1 System Parameters

Parameters	Values
Source Voltage, Frequency & feeder impedance	11KV, Freq-50 Hz & R=3.025ohms, L=57.75 mH
Micro grid load: Impedance load	$R_L=100\text{ohms}$ , $L_L=300\text{Mh}$
DG's & VSC's	$V_{DC-1}=V_{DC-2}=3.5\text{KV}$ ; 3kv/ 11 kv, 0.5 MVA
Transformer rating	$L_1=20\text{Mh}$ , $L_2=16\text{mH}$ ; $L_G=28.86\text{Mh}$

#### ➤ CASE I. Micro Grid Load Exchange of the DG with Main Grid:

If micro grid load power demand is more than generated power by the distribution generation, the rest of power is exchange by the main grid as seen in fig 4.

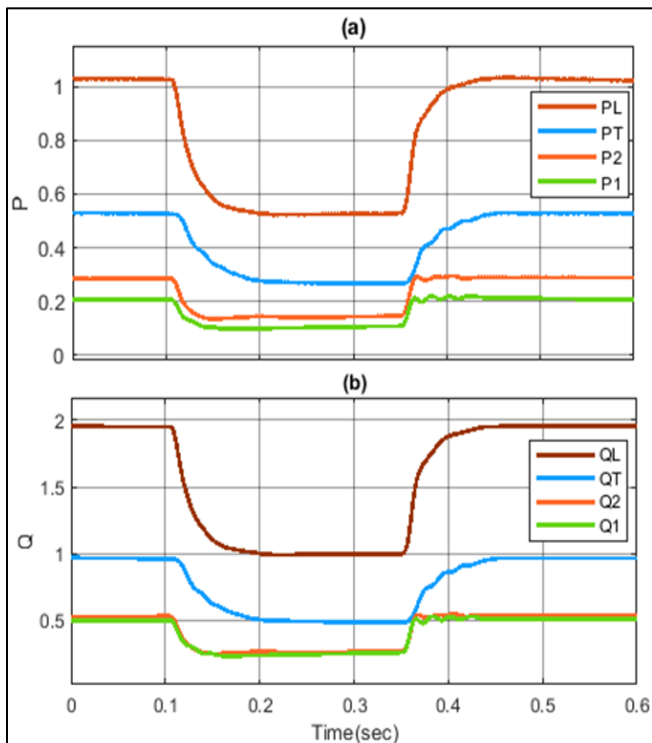


Fig 4 The Power Exchange of True & Reactive Power for Case-I

It is observed that 50 % of load is shared by main grid and remaining load requirements are shared by DG-1 & 2 as seen in fig.4. From fig 5, it is observed that the tracking voltage error is 0.2%. the capacitor voltage  $V_C$  and its angle is at 0.1 sec, the load impedance increased and at 0.35 sec it is changed to its initial value as shown in fig 6.

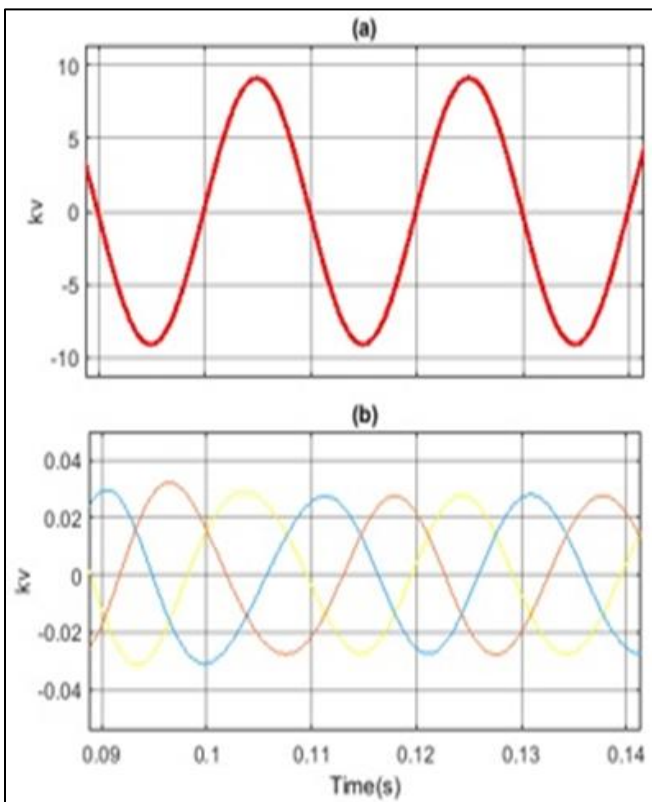


Fig 5 DG-1 Voltage Tracking

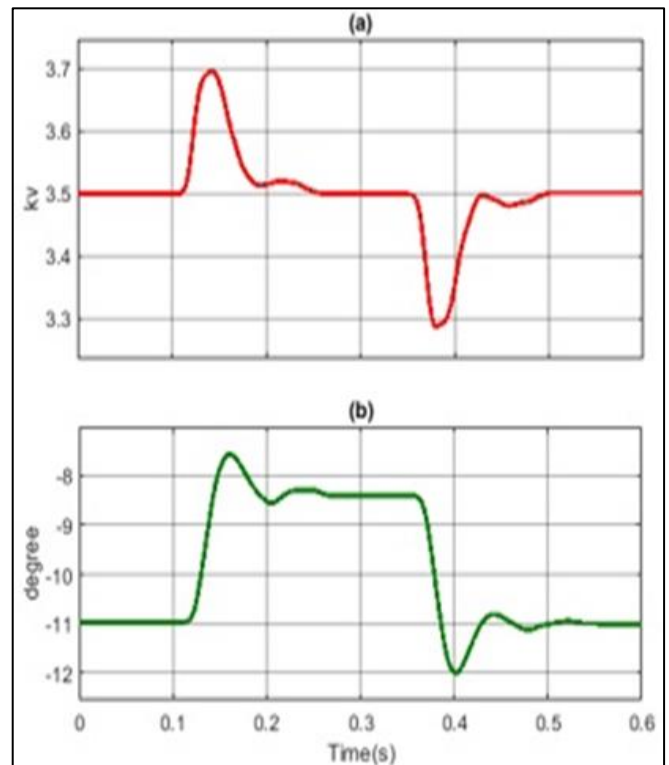


Fig 6 Capacitor Voltage and its Angle Controller

➤ *Case II. Supply Power Change from Main Grid :*

If power flow from main grid to microgrid is changed by changing VSC-2 power flow reference, the remaining required power is taken abruptly by DG's.

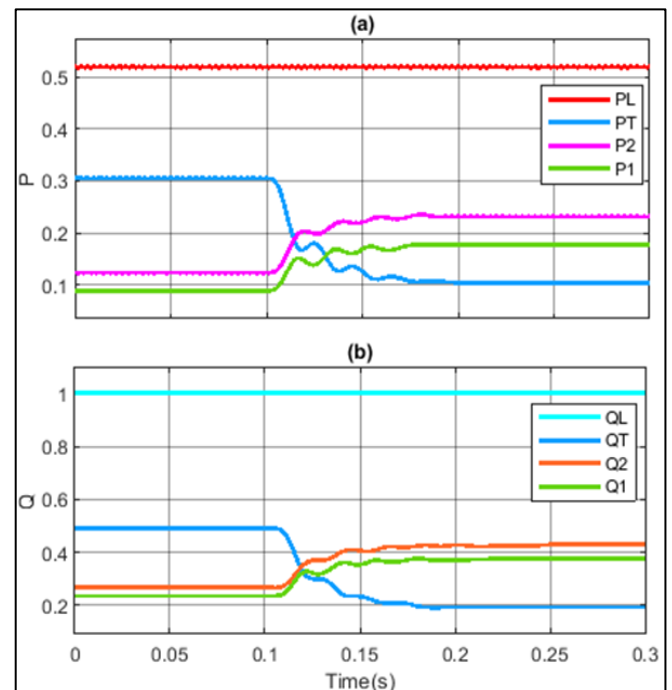


Fig 7 Power Exchange of True Power & Reactive Power for Case II.

Fig 7 shows power exchange of true and reactive power, at 0.1 sec the Power move from main grid is change from 50% of initial load in case-I to 20% of load. And it is observed that DG's pick up the remaining load power & it

shares proportionally. Fig 8 shows the 3-phase point of common coupling voltage & current injected for case-II.

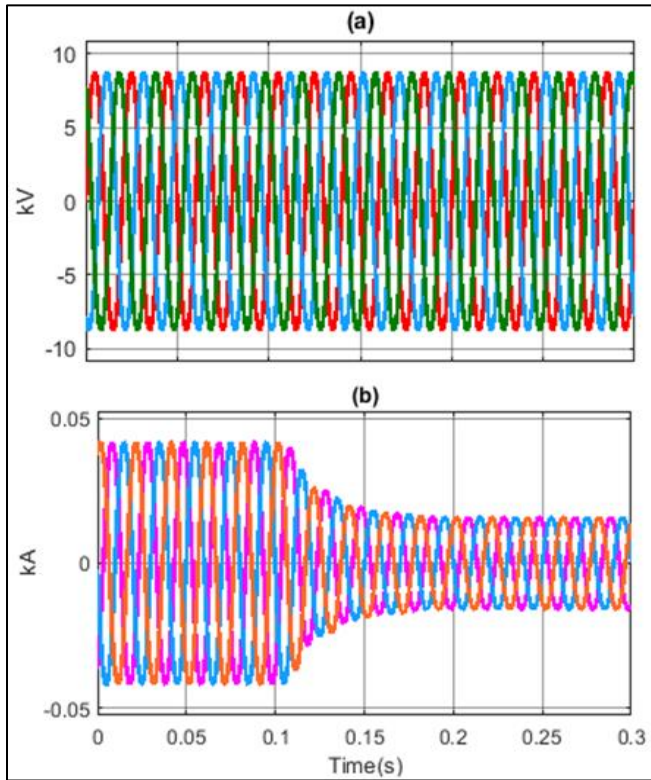


Fig 8 3-phase Voltage at PCC and Current Injectin Case-II.

➤ **CASE-III. Power Delivered from Microgrid to Main Grid:**  
 When load on the system is minimum and distribution generation power is more generated then the balance power is carried back to main grid between back to back voltage source converters is shown in fig9.a

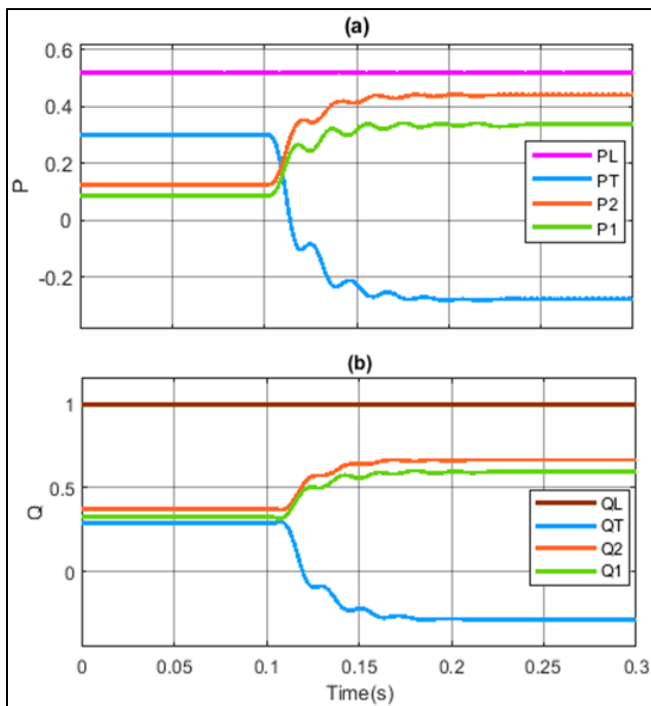


Fig 9. a. The Power Exchange between True Power & Reactive Power for Case-III.

From fig 9.b. Reference grid power are changed and load is increased reference grid power is the from 0 to 0.1 seconds load is 600 KW, 1000 KVar, from 0.1 to 0.35 seconds load is 570 KW, 950 KVar, from 0.35 to 0.6 seconds load is 540 KW, 900KVar, from 0.6 to 0.85 seconds load is 510 KW, 850KVar, after 0.85 seconds load is 420 KW, 700KVar .the true and reactive power sharing as shown in fig 9 b.

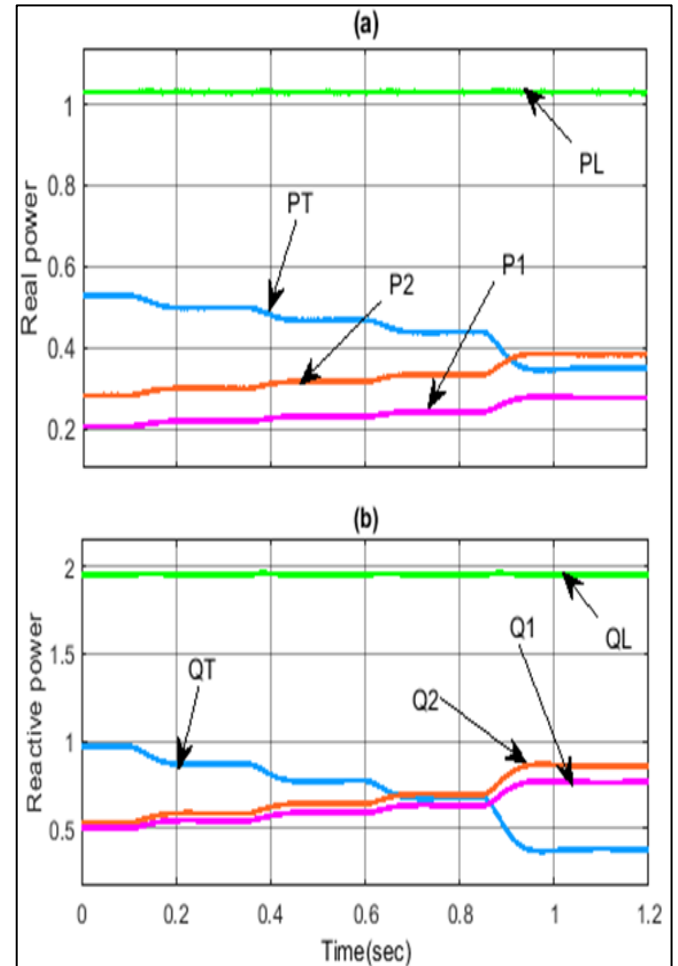


Fig 9.b. Reference Grid Power Changed & Load Increased Reference Grid Power

➤ **Case IV- When the Micro Grid Load is Increased & Decreased i.e. over Load and under Voltage Conditions:**  
 At initial condition( 0-0.1s) the true power load is 100% (100kW) ,at time ( 0.1s to 0.35s) the true power load is increased to 125% , at time (0.35s to 0.6s ) the true power load is increased to 150% , at time ( 0.6s to 0.85s ) the true power load is increased to 200% , at time 0.85s the true power load is reached is in initial positions ,similarly for reactive power sharing as shown in fig 10.

**V. CONCLUSION**

Load exchange between main grid & micro grid is presented in this paper, Active and Reactive power control to achieve proper power sharing under grid connected mode of operation. The power management strategies determine output active & reactive powers of DG's and control the voltages and frequency at same time. Power management system should share the power demand between the existing AC & DC sources by a specified droop method.

**REFERENCES**

- [1]. Kornbluth, Yosef, Gabriel Cwilich, Sergey V. Buldyrev, Saleh Soltan, and Gil Zussman. "Distribution of blackouts in the power grid and the Motter and Lai model." *Physical Review E* 103, no. 3 (2021): 032309.
- [2]. Priyadarshini, I., Mohanty, P., Kumar, R., Son, L.H., Chau, H.T.M., Nhu, V.H., Thi Ngo, P.T. and Tien Bui, D., 2020, May. Analysis of outbreak and global impacts of the COVID-19. In *Healthcare* (Vol. 8, No. 2, p. 148). MDPI.
- [3]. Vargas, R., Macedo, L.H., Home-Ortiz, J.M., Mantovani, J.R.S. and Romero, R., 2021. Optimal restoration of active distribution systems with voltage control and closed-loop operation. *IEEE Transactions on Smart Grid*, 12(3), pp.2295-2306.
- [4]. Shen, W., Chen, X., Qiu, J., Hayward, J.A., Sayeef, S., Osman, P., Meng, K. and Dong, Z.Y., 2020. A comprehensive review of variable renewable energy levelized cost of electricity. *Renewable and Sustainable Energy Reviews*, 133, p.110301.
- [5]. Violante, W., Canizares, C.A., Trovato, M.A. and Forte, G., 2020. An energy management system for isolated microgrids with thermal energy resources. *IEEE Transactions on Smart Grid*, 11(4), pp.2880-2891.
- [6]. Singh, J., Prakash Singh, S., Shanker Verma, K., Iqbal, A. and Kumar, B., 2021. Recent control techniques and management of AC microgrids: A critical review on issues, strategies, and future trends. *International Transactions on Electrical Energy Systems*, 31(11), p.e13035.
- [7]. Vuddanti, S. and Salkuti, S.R., 2021. Review of energy management system approaches in microgrids. *Energies*, 14(17), p.5459.
- [8]. Salehi, N., Martínez-García, H., Velasco-Quesada, G. and Guerrero, J.M., 2022. A comprehensive review of control strategies and optimization methods for individual and community microgrids. *IEEE access*, 10, pp.15935-15955.
- [9]. Solanke, T.U., Khatua, P.K., Ramachandramurthy, V.K., Yong, J.Y. and Tan, K.M., 2021. Control and management of a multilevel electric vehicle's infrastructure integrated with distributed resources: A comprehensive review. *Renewable and Sustainable Energy Reviews*, 144, p.111020.

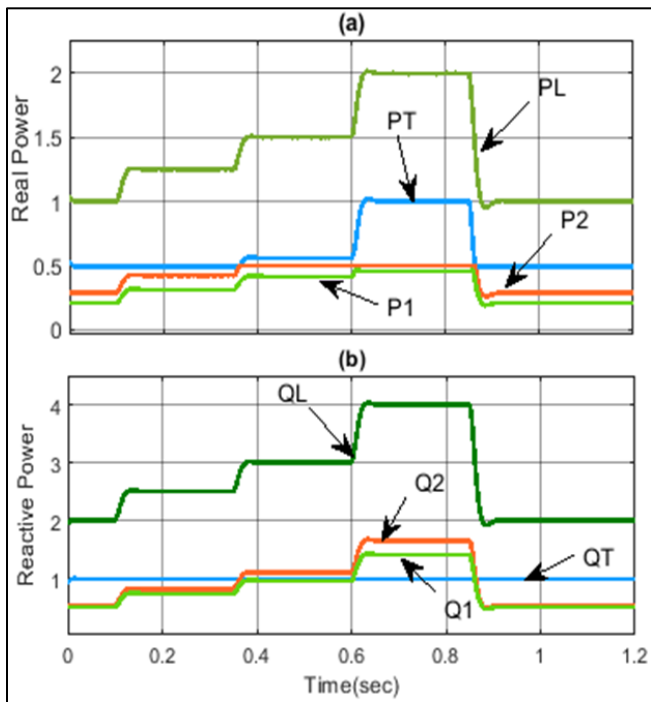


Fig 10 True Power & Reactive Power Exchange when the Micro Grid Load Increment

➤ *Case V- Reactive Power Load Changes with True Power Constant:*

When reactive power load changes by keeping true power constant, power sharing between the main grid & DG's as shown in fig 11. At initial condition(0-0.1s) the reactive power load is 2000kVAR. after 0.1 s it is increased to 25% i.e. 2500kVAR, at time (0.35 to 0.6 s) the reactive power 3000kVAR, then at time 0.6 to 0.85 s reactive power load is increased by 4000kVAR. the true and reactive power sharing as shown in fig11.

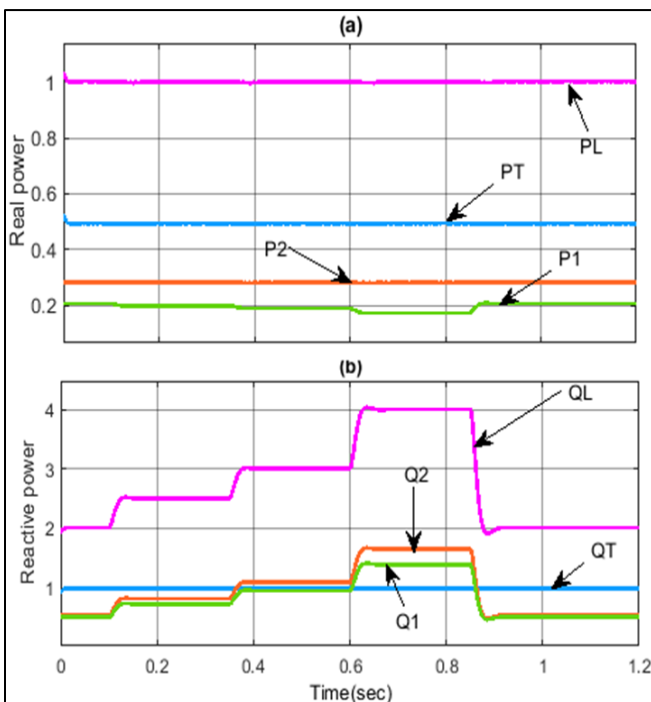


Fig 11 Power Exchange between Main Grid and DG's for Case V



- [10]. Espín-Sarzosa, D., Palma-Behnke, R. and Núñez-Mata, O., 2020. Energy management systems for microgrids: Main existing trends in centralized control architectures. *Energies*, 13(3), p.547.
- [11]. Gulzar, Muhammad Majid, Ayesha Iqbal, Daud Sibtain, and Muhammad Khalid. "An innovative converterless solar PV control strategy for a grid connected hybrid PV/wind/fuel-cell system coupled with battery energy storage." *IEEE Access* 11 (2023): 23245-23259.
- [12]. Lu, Xi, Shiwei Xia, Guangzeng Sun, Junjie Hu, Weiwei Zou, Quan Zhou, Mohammad Shahidehpour, and Ka Wing Chan. "Hierarchical distributed control approach for multiple on-site DERs coordinated operation in microgrid." *International Journal of Electrical Power & Energy Systems* 129 (2021): 106864.
- [13]. Wang, D., Weyen, D. and Van Tichelen, P., 2023. Proposals for Updated EMC Standards and Requirements (9–500 kHz) for DC Microgrids and New Compliance Verification Methods. *Electronics*, 12(14), p.3122.
- [14]. Mosayebi, M., Sadeghzadeh, S.M., Khooban, M.H. and Guerrero, J.M., 2020. Decentralised non-linear I–V droop control to improve current sharing and voltage restoration in DCNG clusters. *IET Power Electronics*, 13(2), pp.248-255.
- [15]. Elgammal, Adel, and Tagore Ramlal. "Adaptive voltage regulation control strategy in a stand-alone islanded DC microgrid based on distributed wind/photovoltaic/diesel/energy storage hybrid energy conversion system." *European Journal of Electrical Engineering and Computer Science* 5, no. 4 (2021): 26-33.
- [16]. Sivadasan, J., Vignesh, R., Antony Robinson, J., Justin Diraviam, J., Senthilkumar, S. and Aandal, R., 2023, May. A switched boost landsman converter with ANFIS based MPPT for grid connected wind energy system. In *AIP Conference Proceedings* (Vol. 2618, No. 1). AIP Publishing.
- [17]. Cao, D., Zhao, J., Hu, W., Ding, F., Huang, Q. and Chen, Z., 2021. Attention enabled multi-agent DRL for decentralized volt-VAR control of active distribution system using PV inverters and SVCs. *IEEE transactions on sustainable energy*, 12(3), pp.1582-1592.
- [18]. Li, D., Wu, Z., Zhao, B. and Zhang, L., 2020. An improved droop control for balancing state of charge of battery energy storage systems in AC microgrid. *IEEE Access*, 8, pp.71917-71929.
- [19]. Pham, M.D. and Lee, H.H., 2020. Effective coordinated virtual impedance control for accurate power sharing in islanded microgrid. *IEEE Transactions on Industrial Electronics*, 68(3), pp.2279-2288.
- [20]. Li, X., Shang, Z., Peng, F., Li, L., Zhao, Y. and Liu, Z., 2021. Increment-oriented online power distribution strategy for multi-stack proton exchange membrane fuel cell systems aimed at collaborative performance enhancement. *Journal of Power Sources*, 512, p.230512.
- [21]. Jiang, E., Zhao, J., Shi, Z., Mi, Y., Lin, S. and Muyeen, S.M., 2023. Intelligent Virtual Impedance Based Control to Enhance the Stability of Islanded Microgrid. *Journal of Electrical Engineering & Technology*, 18(5), pp.3971-3984.
- [22]. Pham, X.H.T., 2020. Power sharing strategy in islanded microgrids using improved droop control. *Electric Power Systems Research*, 180, p.106164.